A Mutation in the *C. elegans* EXP-2 Potassium Channel That Alters Feeding Behavior

M. Wayne Davis,[1]*† Richard Fleischhauer,[2] Joseph A. Dent,[1]‡ Rolf H. Joho,[2] Leon Avery[1]

The nematode pharynx has a potassium channel with unusual properties, which allows the muscles to repolarize quickly and with the proper delay. Here, the *Caenorhabditis elegans exp-2* gene is shown to encode this channel. EXP-2 is a Kv-type (voltage-activated) potassium channel that has inward-rectifying properties resembling those of the structurally dissimilar human *ether-à-go-go*–related gene (HERG) channel. Null and gain-of-function mutations affect pharyngeal muscle excitability in ways that are consistent with the electrophysiological behavior of the channel, and thereby demonstrate a direct link between the kinetics of this unusual channel and behavior.

Byerly and Masuda (*1*) were the first to describe an unusual K^+ current in the pharyngeal muscles of *Ascaris lumbricoides*. They called this current the negative spike current because it mediates negative-going spikes from depolarized potentials in current-clamped pharyngeal muscles. The negative spike channel has properties reminiscent of the HERG K^+ channel that mediates the I_{Kr} current in the heart. Subsequently, current-clamp studies have shown that the *C. elegans* pharyngeal muscle has similar repolarization kinetics to those of *Ascaris* (*2*), suggesting that *C. elegans* also has this unusual K^+ channel.

The original, semidominant *exp-2(sa26)* allele was isolated in a screen for worms with defective defecation behavior (*3*). Animals heterozygous for the gain-of-function *exp-2* allele had hyperactive head movements, defective egg laying, and brief, shallow pharyngeal contractions. Homozygotes arrested as newly hatched larvae and eventually died, probably because they do not eat.

To examine the null phenotypes of *exp-2*, we isolated several *exp-2(sa26)* revertant alleles (*4*). Each of these alleles was recessive, homozygous viable, and caused no obvious defects in defecation (*5*) or in head movement. Instead of brief pharyngeal muscle contractions, null mutants had long-lasting pharyngeal muscle contractions that could last several seconds (*6*).

Wild-type pharyngeal action potentials begin with a rapid depolarization to +20 to +35 mV (*7*) and have a slowly declining plateau phase that lasts around 150 to 250 ms (Fig. 1). At the end of the action potential, there was a rapid hyperpolarization that reached approximately −70 mV followed by a slow depolarization to rest (around −40 mV). In *exp-2* gain-of-function heterozygotes, depolarization was normal. However, the plateau phase was very brief, ending with a rapid hyperpolarization about 70 ms after depolarization. Furthermore, the membrane potential between action potentials was near −70 mV. The *exp-2* loss-of-function pharynxes had normal interpump membrane potentials, and their action potentials had normal depolarization and normal plateau phases for the first 150 ms (Fig. 1) (*7*). However, instead of a rapid repolarization at the end of this period, the potential slowly oscillated near 0 mV for up to 7 s (Fig. 1). After this, the membrane slowly hyperpolarized with little or no overshoot.

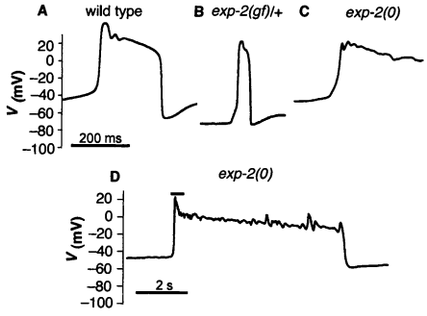

Fig. 1. Action potentials from wild-type and *exp-2* mutant pharyngeal muscles. (**A**) Wild-type, (**B**) gain-of-function *exp-2(sa26)/+*, and (**C**) null *exp-2 (ad1426)* action potentials. (**D**) The null mutant action potential on a contracted time scale. The bar above the initial part of the action potential indicates the portion of the action potential shown in (C).

We placed *exp-2* between cosmids ZC250 and W06H8 by mapping with respect to deficiencies with known molecular break points (*8*). We found a gene on the cosmid F12F3 (*9*), which lies between ZC250 and W06H8, that appeared to encode a K^+ channel. We rescued the *exp-2* loss-of-function pharyngeal action-potential defect with a polymerase chain reaction (PCR) product containing only the promoter and coding region of a putative K^+ channel from cosmid F12F3, demonstrating that this gene is likely to be *exp-2* (*10*). We sequenced the K^+ channel coding region from several *exp-2* alleles (*11*) and found that the gain-of-function allele, *sa26,* was a Cys-to-Tyr mutation in the S6 segment of the K^+ channel (*12*). Most of the loss-of-function alleles are in the highly conserved pore domain (*12*), and all but *ad1559* appear to be null (*13*). Comparison of the *exp-2* coding sequence with those of other K^+ channel genes showed that *exp-2* is a member of the six-transmembrane, voltage-activated (Kv-type) family of K^+ channels (*12*).

We fused a 4047–base pair length of the *exp-2* promoter and most of the *exp-2* coding region to green fluorescent protein (GFP). In transgenic worms, the GFP fusion protein was expressed strongly in pharyngeal muscle

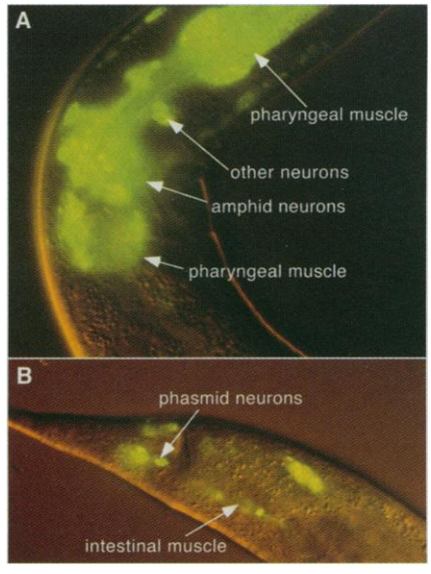

Fig. 2. Expression pattern of an *exp-2*::GFP reporter fusion. GFP fused to the COOH-terminus of *exp-2* is strongly expressed in (**A**) the pharyngeal muscle and amphid neurons in the anterior portion of the worm and (**B**) phasmid neurons and the intestinal muscle in the posterior portion of the worm. The *exp-2*::GFP fusions contain the *exp-2* promoter and coding regions encoded by an Nae I to Sal I fragment from the cosmid F12F3 fused to a Sal I to Apa I fragment from pPD95.77 (gift from A. Fire, J. Ahnn, G. Seydoux, and S. Xu) containing GFP coding sequences and the *unc-54* 3′ untranslated region.

[1]Department of Molecular Biology, University of Texas Southwestern Medical Center, Dallas, TX 75390–9148, USA. [2]The Center for Basic Neuroscience, University of Texas Southwestern Medical Center, Dallas, TX 75390–9111, USA.

*Present address: Department of Biology, University of Utah, Salt Lake City, UT 84112–0840, USA.
†To whom correspondence should be addressed. E-mail: wdavis@biology.utah.edu
‡Present address: Department of Biology, McGill University, Montreal, PQ H3A 1B1, Canada.

(Fig. 2A), in the intestinal muscles (Fig. 2B), and occasionally faintly in the egg-laying muscles (*14*). Each of these muscle types was affected by the gain-of-function *exp-2* mutation. The reporter was also expressed in several neurons of the nerve ring ganglia (Fig. 2A). The amphid neurons are the primary chemosensory neurons of the animal, so disrupting their normal excitability would explain the chemotaxis defect seen in *exp-2* loss-of-function animals (*15*).

We expressed in vitro–transcribed EXP-2 complementary RNA (cRNA) in *Xenopus laevis* oocytes (*16*). Oocytes were held at −80 mV, and 1-s depolarizing pulses were applied, followed by 200-ms pulses to −120 mV (Fig. 3A). We saw no outward currents, but saw large inward-directed tail currents during the 200-ms pulse to −120 mV following pulses to −30 mV or higher (Fig. 3A). The tail currents did not appear instantaneously but showed a rising phase, indicating time-dependent recovery from inactivation. The magnitude of these currents increased with increasing extracellular K^+ concentration, and the zero current level was close to E_K, indicating that oocyte-expressed EXP-2 channels are potassium selective (*17*). The peak levels of the tail currents had a midpoint of activation ($V_{0.5}$) at −17 ± 2 mV (mean ± SEM, n = 5) (Fig. 3D). The voltage-dependent activation of EXP-2 channels during the test pulse occurred relatively slowly at +20 mV with an activation time constant of 54 ± 5 ms (mean ± SEM, n = 10 oocytes) (*17*).

Oocytes expressing the $Cys^{480} \rightarrow Tyr^{480}$ (C480Y) mutant cRNA showed relatively large inward currents that increased at more negative holding potentials (Fig. 3B). Depolarizing 1-s pulses to potentials more positive than −50 mV appeared to activate additional channels because there was a small increase in the subsequent tail currents at −140 mV. Hence, it appeared that the C480Y mutation in S6 prevented the majority of channels from closing, even at potentials as negative as −160 mV.

We co-injected wild-type EXP-2 and C480Y mutant cRNA (at a 1:1 ratio) to model the channel composition in heterozygous worms that show very brief action potentials (Fig. 3C). We saw some inward currents that increased at more negative potentials (from −80 to −140 mV). These inward currents were probably caused by a small fraction of homotetrameric C480Y mutant channels. The first inward tail current appeared around −70 mV, indicating the formation of K^+ channels with novel properties (presumably heterotetramers) that open at more negative potentials ($V_{0.5}$ = −30 ± 4 mV; mean ± SEM, n = 4) (Fig. 3D).

The C480Y mutation, which apparently uncouples channel opening from voltage-dependent gating in EXP-2, is located in S6 close to a position involved in C-type inactivation in Shaker (A463) (*18*) and Kv1.3 (A413) (*19*) and a position in Kv2.1 (C393) involved in stabilizing the open state (*20*). We used the crystal structure of the KcsA K^+ channel (*21*) as a scaffold to generate a three-dimensional model of the EXP-2 pore, including the transmembrane segments S5 and S6, to understand how the structural change in the C480Y mutant traps the channel in the open state at more negative membrane potentials (*22*). The large Tyr side chain in the C480Y mutant protrudes from S6 to near S5 (Fig. 4). In contrast, the smaller side chain of Cys is buried close to S6. It has been suggested that S6 needs to rotate counterclockwise (viewed from the outside) for the KcsA channel to open (*23*). If EXP-2 is similarly gated, the rotation of S6 would move the

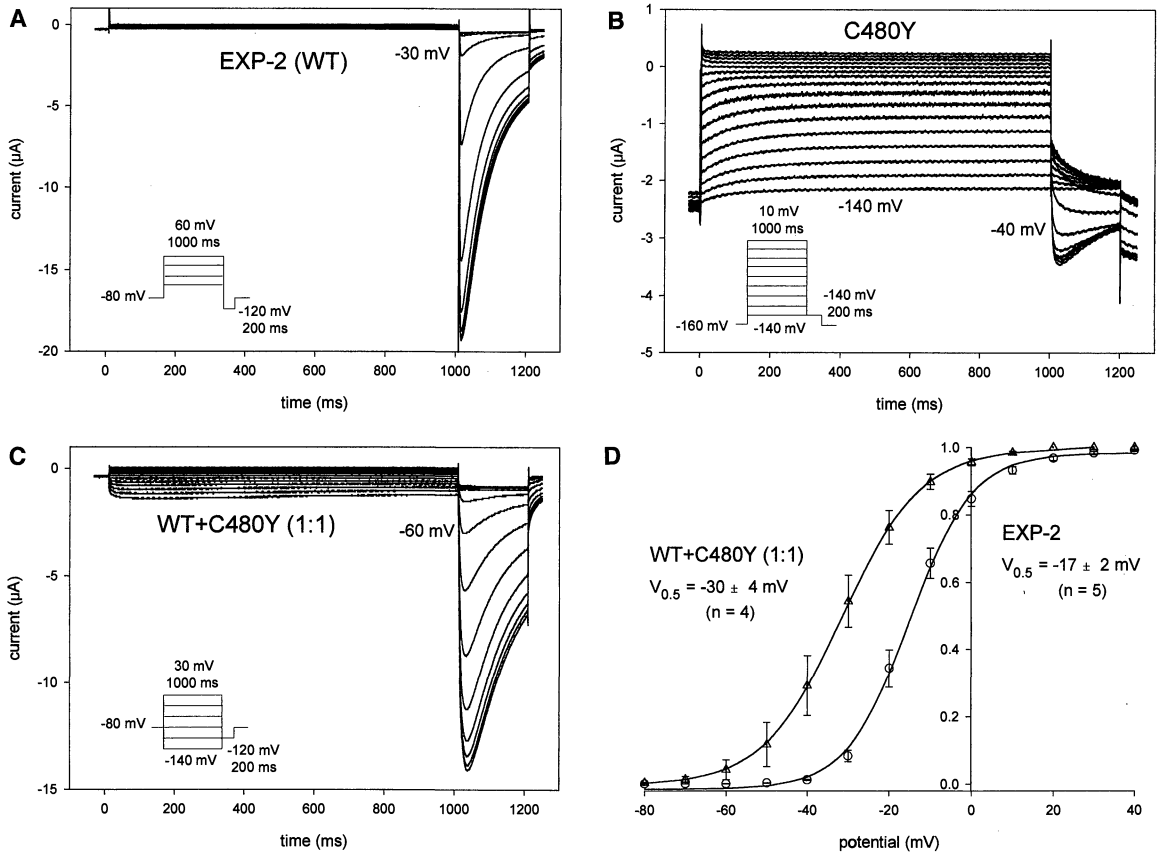

Fig. 3. Voltage dependence of EXP-2 and S6 mutant C480Y channels. Oocytes were subjected to a two-electrode voltage-clamp protocol in a modified frog Ringer solution containing 100 mM KCl to facilitate the measurement of inward and outward K^+ currents. **(A)** Oocytes were held at −80 mV. We applied 1-s depolarizing pulses to potentials from −60 to +60 mV in 10-mV increments, followed by a 200-ms pulse to −120 mV. During a pulse to −30 mV, EXP-2 channels become measurably activated, as seen by the inward tail current during the 200-ms pulse to −120 mV. **(B)** Oocytes expressing the C480Y mutant show inward K^+ currents at potentials as negative as −160 mV, indicating the presence of constitutively open channels. Strong depolarization (positive to ~−40 mV) appears to open additional channels, as seen by the increasing tail currents at −140 mV. We never saw inward currents of this magnitude, either in uninjected (data not shown) or in oocytes injected with wild-type EXP-2 cRNA (A). **(C)** Co-injection of wild-type and C480Y cRNA generates putative heterotetrameric channels with novel properties. Most channels are closed at a holding potential of −80 mV but begin to activate at ~−70 mV. **(D)** Conductance-voltage relationship for wild-type EXP-2 and the C480Y mutant heterotetramer. The midpoint of activation and the apparent activation threshold are shifted to hyperpolarized potentials by 13 and ~30 mV, respectively, in the C480Y mutant heterotetramer.

bulky Tyr side chain away from the S5 helix on opening, relieving the unfavorable steric interaction. Thus, the mutation would tend to shift the equilibrium toward the open state, as observed.

The physiological role of EXP-2 channels in the pharynx is reminiscent of the behavior of HERG channels in the vertebrate heart; both EXP-2 and HERG channels act to repolarize the muscle after a long action potential. The channels have similar kinetics: slow voltage-dependent activation followed by fast inactivation [inactivation in EXP-2 is even faster than in HERG (*17*)]. However, EXP-2 and HERG do not have similar amino acid sequences. EXP-2 is a member of the Kv family of K^+ channels, while HERG is a member of the *ether-à-go-go* (*eag*) family of K^+ channels. Thus, it is likely that these channels convergently evolved to serve similar functions.

Here, we describe a mutation that goes all the way from gene to its effect on behavior. First, we characterized the channel at the molecular level. We identified a novel channel gene, and a point mutation that alters its kinetics. The crystal structure of a K^+ channel pore domain (*21*) and electron paramagnetic resonance spectroscopy studies of K^+ channel gating movements (*23*) allowed us to make a plausible argument for how this sequence change leads to the observed changes in channel kinetics. Second, we characterized the biophysical properties of the wild-type and mutant channel in *Xenopus* oocytes. This allowed us to determine the kinetics of the channel in isolation and make predictions about its effects on muscle physiology. Finally, our electrophysiological studies in wild-type, null, and gain-of-function *exp-2* animals showed how the properties of the channel contribute to the physiology of the muscle. The *exp-2* null mutants had no noticeable defect in the action potential until the point when the EXP-2 channel should open and rapidly repolarize the muscle. When the channel was mutated in a way that changed its kinetics, we saw corresponding changes in muscle physiology and behavior. Thus, *exp-2* links channel sequence to channel kinetics, and channel kinetics to muscle physiology. Understanding the connection between genes and behavior in molecular detail is one of the ultimate goals of neurobiology; *exp-2* demonstrates that this goal can be reached.

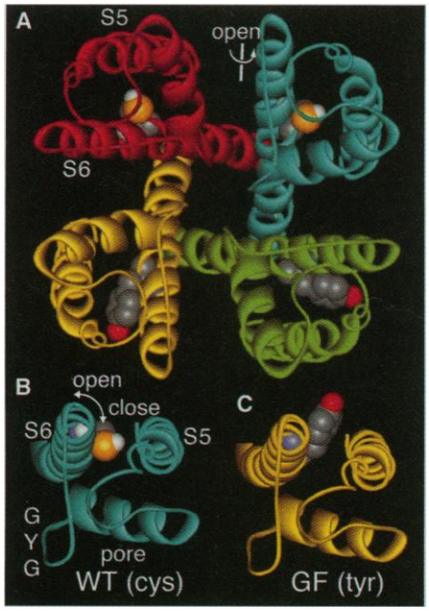

Fig. 4. Location of residue 480 in the three-dimensional structure of EXP-2. A top view of (**A**) a channel heterotetramer (from the outside) and a view straight down S6 (also from the outside) of (**B**) a wild-type subunit and of a (**C**) C480Y subunit with a CPK (Corey-Pauling-Koltun) representation of the Cys and Tyr residues at position 480. These views of the putative closed state of the channel suggest how the Tyr side chain could promote the counterclockwise rotation of S6 that may be required for channel opening.

References and Notes

1. L. Byerly and M. O. Masuda, *J. Physiol. (London)* **288**, 263 (1979).
2. M. W. Davis *et al.*, *J. Neurosci.* **15**, 8408 (1995).
3. J. H. Thomas, *Genetics* **124**, 855 (1990).
4. Worms were cultured and handled as described by J. Sulston and J. Hodgkin [in *The Nematode* Caenorhabditis elegans, W. B. Wood, Ed. (Cold Spring Harbor Laboratory Press, Plainview, NY, 1988), pp. 587–606] with minor modifications as described [L. Avery, *Genetics* **133**, 897 (1993)]. Revertant alleles of *exp-2(sa26)* were isolated after ethyl methane sulfonate mutagenesis by looking for animals that no longer displayed *exp-2(sa26)* gain-of-function head movement or pharyngeal pumping phenotypes. We isolated *exp-2(ad1201)* and *exp-2(ad1426)* using DA1200 and DA1315 *exp-2(sa26sd)/unc-46(e177) sDf44 dpy-11(e224) V* as the starting strain. All other revertant alleles were isolated using DA1090 *exp-2(sa26sd) dpy-11(e224)/unc-46(e177) sDf30 V; mnDp26* as the starting strain.
5. J. Thomas, personal communication.
6. M. W. Davis, J. A. Dent, L. Avery, data not shown.
7. Pharyngeal muscle voltage recordings were done and data analyzed as described (*2*). Pharynxes were dissected into Dent's saline. Cells were penetrated with 0.5 M or 3 M KOAc-filled electrodes (74 to 340 megohms) and potentials recorded with an Axoclamp amplifier. We analyzed 100-s sections of each record for action potential parameters and resting potential. The gain-of-function records were made from DA1090 animals, and loss-of-function records from DA1201, DA1426, and DA1482 *unc-13(e51) eat-11(ad541) I; exp-2(sa26sd ad1426) V* animals. Average parameter values were (mean ± SEM): wild-type (n = 7) peak = +34 ± 3 mV (*2*), overshoot = −67 ± 2 mV (*2*), interpump potential = −45 ± 1 mV (*2*); gain-of-function heterozygote (n = 5) peak = +25 ± 4 mV, duration = 72 ± 10 ms, interpump potential −71 ± 3 mV; loss-of-function (n = 4) peak = +34 ± 4 mV, duration = 3.8 ± 1.3 s, interpump potential −40 ± 3 mV.
8. C. Malone, personal communication.
9. The *C. elegans* Sequencing Consortium, *Science* **282**, 2012 (1998).
10. The *exp-2* loss-of-function worms were transformed [C. C. Mello, J. M. Kramer, D. Stinchcomb, V. Ambros, *EMBO J.* **10**, 3959 (1991)] with a PCR product that began 3.4 kb 5′ to the initiating methionine and ended 854 bases 3′ to the stop codon of *exp-2* (primers: 5′-CCGGATCCGAAAAATGATACGAGCAT-3′ and 5′-CTGCGGCCGGGCCCTTCAATGCCAGAATGCT-3′) using *rol-6(d)* as the co-transformation marker (*2*). Rescue of the *exp-2* action potential defect was confirmed by electropharyngeogram [D. M. Raizen and L. Avery, *Neuron* **12**, 483 (1994)], and rescue of the pharyngeal motion defect was confirmed by direct observation.
11. PCR products that included the entire *exp-2* coding region were generated using a single-worm PCR protocol [B. D. Williams, in Caenorhabditis elegans: *Modern Biological Analysis of an Organism*, H. F. Epstein and D. C. Shakes, Eds. (Academic Press, San Diego, CA, 1995), vol. 48, pp. 81–96] and were used as sequencing templates. The products from at least three independent PCR reactions were mixed before sequencing in order to limit the possibility of detecting PCR-induced mutations. Automated sequencing was done using ABI Prism Big-Dye Terminator cycle sequencing–ready reaction kits and an ABI Prism 377 machine.
12. A supplementary figure, which shows an alignment of the exp-2 sequence with *Drosophila* Kv channels, can be found at the *Science* Web site (www.sciencemag.org/feature/data/1044897.shl).
13. All of the putative null alleles are fully recessive and are phenotypically indistinguishable from each other. Moreover, all are indistinguishable from *ad1573*, an in-frame deletion of the entire S5 transmembrane helix. Because such a protein would be unable to place the K^+ selectivity filter on the correct side of the membrane, this mutation is a likely molecular null.
14. M. W. Davis, data not shown.
15. S. Owens, J. Pierce, S. Lockery, personal communication.
16. Reverse transcription–PCR (using the primers 5′-CUACUACUACATATGGCGATTGCAATATCGCAA-3′ and 5′-CAUCAUCAUCAUGCTAGCGAGTTTCCCGTTGAAATTGGA-3′) was used to generate a full-length *exp-2* cDNA. This was inserted into the pT7 expression vector (a derivative of pSP64) [R. B. Cary *et al.*, *J. Cell Sci.* **107**, 1609 (1994)], and its sequence confirmed by sequencing. The gain-of-function *exp-2(sa26)* mutation was introduced into the pT7::cDNA construct by PCR mutagenesis and was then confirmed by sequencing. In vitro transcription was done using a Ribomax T7 kit. Oocyte recordings were done and analyzed as described [R. D. Zühlke, H. J. Zhang, R. H. Joho, *Receptors Channels* **2**, 237 (1994)]. Approximately 1 to 3 ng cRNA was injected into *Xenopus* oocytes, and 2 to 4 days after injection, the cells were subjected to two-electrode voltage-clamp [A. M. VanDongen, G. C. Frech, J. A. Drewe, R. H. Joho, A. M. Brown, *Neuron* **5**, 433 (1990)]. To facilitate the recording of inward current, experiments were done in a bath solution containing high KCl [100 mM KCl, 1.0 mM $MgCl_2$, 1.8 mM $CaCl_2$, 5 mM HEPES (pH 7.5) at 22°C ± 1°C].
17. R. Fleischhauer *et al.*, *J. Neurosci.*, in press.
18. T. Hoshi, W. N. Zagotta, R. W. Aldrich, *Neuron* **7**, 547 (1991).
19. G. Panyi, Z. Sheng, C. Deutsch, *Biophys. J.* **69**, 896 (1995).
20. Y. Liu and R. H. Joho, *Pfluegers Arch. Eur. J. Physiol.* **435**, 654 (1998).
21. D. A. Doyle *et al.*, *Science* **280**, 69 (1998).
22. The crystal structure of the bacterial KcsA channel (Protein Data Bank entry 1BL8) (*21*) was used as the modeling template. KcsA displays a high degree of sequence similarity to EXP-2 and other Kv-type K^+ channels near and in the pore region. The program Swiss-PDB Viewer was used to align the primary sequences and to prepare the files necessary for processing by the Swiss-MODEL server [N. Guex and M. C. Peitsch, *Electrophoresis* **18**, 2714 (1997)] (www.expasy.ch/swissmod/SWISS-MODEL.html). The Swiss-MODEL server is an automated system that generates an alignment between the sequence of a known structure and the sequence to be modeled,

generates a model structure for the new sequence based on the experimentally determined structure, and refines the model sequence using energy minimization and molecular dynamics. Swiss-PDB Viewer was used to generate the Cys-to-Tyr mutant structure, by replacement of the side chain and selection of the lowest energy rotamer. WebLab ViewerLite (www.msi.com/weblab/index.html) was used to manipulate the resulting models and prepare images for presentation.

23. E. Perozo, D. M. Cortes, L. G. Cuello, *Science* **285**, 73 (1999).

24. We would like to thank D. Hilgemann, R. Lin, and D. Smith for critical comments on the manuscript, A. Chiang for assistance in screening for *exp-2(sa26)* revertants, and A. Fire, J. Ahnn, G. Seydoux, and S. Xu for the gift of pPD95.77. Some strains were received from the *Caenorhabditis* Genetics Center, which is funded by the NIH National Center for Research Resources. J. Thomas kindly provided us with the *exp-2(sa26)* allele. Supported by NIH grants HL46154 to L.A. and NS28407 to R.H.J.

26 August 1999; accepted 16 November 1999

Inattentional Blindness Versus Inattentional Amnesia for Fixated But Ignored Words

Geraint Rees,[1,2]* Charlotte Russell,[3] Christopher D. Frith,[1] Jon Driver[3]

People often are unable to report the content of ignored information, but it is unknown whether this reflects a complete failure to perceive it (inattentional blindness) or merely that it is rapidly forgotten (inattentional amnesia). Here functional imaging is used to address this issue by measuring brain activity for unattended words. When attention is fully engaged with other material, the brain no longer differentiates between meaningful words and random letters, even when they are looked at directly. These results demonstrate true inattentional blindness for words and show that visual recognition wholly depends on attention even for highly familiar and meaningful stimuli at the center of gaze.

The extent of processing for unattended objects has been debated for over four decades (*1*). Recognition of unattended words is considered a crucial test case (*1–3*), because for these visual stimuli the processing of higher order cognitive properties (such as identity and meaning) can be dissociated from mere visual appearance. Early findings of little awareness or memory for ignored words (*4*) were taken to support the hypothesis that word recognition depends on attention. However, other studies suggested that word recognition still may take place unconsciously or implicitly for ignored words (*5, 6*), which led to proposals that word recognition is fully automatic (*2, 7*).

Functional imaging provides a way to measure unattended processing, but until now it has not been applied to the classic issue of the level of processing for unattended words. Recent data show that attention can modulate the activity evoked by visual stimuli within early brain areas (*8*), but all the stimuli used were meaningless or unfamiliar (for example, flashes, colored grids, or moving dots) and so cannot resolve the issue of unattended processing for meaningful familiar stimuli such as ignored words. Moreover, existing brain imaging data suggest that unattended processing may be attenuated rather than completely eliminated at early levels of processing, so processing of an unattended stimulus still may proceed through to higher levels beyond a rudimentary analysis of physical features (*9*). Here we resolve these issues by showing that brain activity in response to familiar visual words, versus random letters, wholly depends on attention.

We created a situation in which people could look directly at a word without attending to it (*10*). Brain activity was measured with functional magnetic resonance imaging (fMRI) (*11*) as participants viewed displays of a rapid stream of letter strings superimposed on a rapid stream of pictures (Fig. 1). The letter stream either consisted of meaningless strings of random consonants or contained a high proportion of meaningful familiar words. At any one time, participants attended only the stream of letters or only the superimposed stream of pictures in order to detect any immediate repetition of a stimulus within the attended stream. We arranged the stimulus parameters so that monitoring one stream for repetition was sufficiently demanding to preclude any attention to the other stream (*10*), even though both were superimposed at fixation. When the stream of letters was attended, we expected meaningful words within it to activate the extensive left-hemisphere network identified in previous imaging studies of word processing (*12*). The new question was whether meaningful words would similarly produce differential brain activation when the letter strings were ignored, with the superimposed pictures being attended instead. If true inattentional blindness can arise for ignored words, then activation for words versus nonwords should no longer be found. By contrast, if word processing is fully automatic, as is often argued to be the case (*2, 7, 13*), then differential activation still should be found even for ignored words because they are automatically perceived, with any effects of inattention being more akin to inattentional amnesia (*14*) than to inattentional blindness (*15*).

Immediately after scanning, participants underwent surprise recognition memory tests for the meaningful words they had been shown (*16*). Although recognition memory was excellent for those words that appeared in an attended stream, ignored words were not distinguished from new words (Fig. 1, bottom). This confirms that our manipulation of attention was psychologically effective and agrees with previous findings that people cannot recognize the identity of unattended stimuli retrospectively (*17*).

First we compared brain activations when participants were attending to the picture streams versus the letter streams overall (*18*). The stimuli were identical for these comparisons, as were the motor responses when detecting repetition, so any differential brain response must be due to what was attended. Attending to pictures compared with letter strings activated an extensive network of ventral visual areas bilaterally (Fig. 2A, green), whereas attending to letter strings compared with pictures activated a left occipital region (Fig. 2A, red) previously associated with letter perception (*19*). These activations indicate that covert attention can substantially affect neural responses in the visual system even when attended and ignored stimuli are spatially superimposed.

The crucial test for brain responses to meaningful familiar words compares the activation evoked by words versus consonants within the letter stream. When the letter stream was attended, words minus consonants revealed strong activity in a left-lateralized network of areas, including posterior basal temporal, parietal, and prefrontal cortex (Fig. 2B and Table 1). This is consistent with previous lesion and functional imaging studies of word processing (*12, 13, 20*). Because words differ from consonant strings in several respects (for example, legal orthography and phonology, lexical status, semantics), the

[1]Wellcome Department of Cognitive Neurology, Institute of Neurology, University College London, 12 Queen Square, London WC1N 3BG, UK. [2]Division of Biology 139-74, California Institute of Technology, Pasadena, CA 91125, USA. [3]Institute of Cognitive Neuroscience, Department of Psychology, University College London, 17 Queen Square, London WC1N 3AR, UK.

*To whom correspondence should be addressed. E-mail: geraint@klab.caltech.edu

References and Notes

[9] **Genome Sequence of the Nematode C. elegans: A Platform for Investigating Biology**
The C. elegans Sequencing Consortium
Science, New Series, Vol. 282, No. 5396. (Dec. 11, 1998), pp. 2012-2018.
Stable URL:
http://links.jstor.org/sici?sici=0036-8075%2819981211%293%3A282%3A5396%3C2012%3AGSOTNC%3E2.0.CO%3B2-M

[21] **The Structure of the Potassium Channel: Molecular Basis of K⁺ Conduction and Selectivity**
Declan A. Doyle; João Morais Cabral; Richard A. Pfuetzner; Anling Kuo; Jacqueline M. Gulbis; Steven L. Cohen; Brian T. Chait; Roderick MacKinnon
Science, New Series, Vol. 280, No. 5360. (Apr. 3, 1998), pp. 69-77.
Stable URL:
http://links.jstor.org/sici?sici=0036-8075%2819980403%293%3A280%3A5360%3C69%3ATSOTPC%3E2.0.CO%3B2-G

[23] **Structural Rearrangements Underlying K⁺-Channel Activation Gating**
Eduardo Perozo; D. Marien Cortes; Luis G. Cuello
Science, New Series, Vol. 285, No. 5424. (Jul. 2, 1999), pp. 73-78.
Stable URL:
http://links.jstor.org/sici?sici=0036-8075%2819990702%293%3A285%3A5424%3C73%3ASRUKAG%3E2.0.CO%3B2-S